6. Both the formation and dissociation kinetics of the Cu^{II}([14]aneN$_2$S$_2$) complex are found to be extremely sluggish in strongly acidic solution where the terms involving two hydrogen ions are presumed to predominate. This phenomenon is attributed to the difficulty in inverting a coordinated nitrogen during the stepwise bonding and dissociation process and should influence all similar macrocyclic ligands involving two nitrogens separated by an ethylene linkage.

Acknowledgment. We express our appreciation to Wayne State University for a Rumble Graduate Fellowship awarded to V.B.P. and to the Research Corp. and the University of Wisconsin-Eau Claire Research and Creativity Fund for grants to L.A.O. in support of portions of this work. Partial support provided to D.B.R. by the National Institutes of Health under Grant GM 20424 and the Getty Conservation Institute is also acknowledged.

Registry No. [14]aneN$_2$S$_2$, 87939-30-8; [14]aneNSSN, 87939-29-5; [14]aneNS$_3$, 87939-28-4; [14]aneNSNS, 55702-76-6; [15]aneNS$_4$, 116319-25-6; [15]aneN$_2$S$_3$, 78988-82-6; [14]aneN$_3$S, 87939-31-9; Cu, 7440-50-8.

Supplementary Material Available: Seven tables containing resolved formation rate constant (k_f) values as a function of pH for the seven systems studied and text describing additional information about the tables (5 pages). Ordering information is given on any current masthead page.

Contribution from the Department of Chemistry,
University of Pittsburgh, Pittsburgh, Pennsylvania 15260

Evaluation of the π-Bonding Ability of Imidazole: Structure Determination and Characterization of *catena*-$(H_2O)_2(1\text{-}CH_3im)_2Mg(\mu\text{-}CN)(CN)_4(1\text{-}CH_3im)Fe^{III}\cdot H_2O$ ($1\text{-}CH_3im$ = 1-Methylimidazole)[1]

Craig R. Johnson, Colleen M. Jones,† Sanford A. Asher,* and Jaime E. Abola

Received February 27, 1990

The preparation of *catena*-diaquabis(1-methylimidazole)magnesium(II)-μ-cyanotetracyano(1-methylimidazole)ferrate(III) monohydrate (**3**) is reported. Crystals of *catena*-$[Mg(H_2O)_2(1\text{-}CH_3im)_2(\mu\text{-}CN)Fe(CN)_4(1\text{-}CH_3im)]\cdot H_2O$ ($1\text{-}CH_3im$ = 1-methylimidazole) are monoclinic, space group $P2_1$, with a = 8.471 (2) Å, b = 15.678 (4) Å, c = 9.722 (2) Å, V = 1190.5 (4) Å^3, Z = 2, and R (R_w) = 0.026 (0.029) for 2104 reflections. The structure contains $(CN)_5Fe(1\text{-}CH_3im)^{2-}$ units linked in extended chains through bridging cyanides (cis to $1\text{-}CH_3im$), which are coordinated to the Mg^{2+} counterions. Two N(CN^-), two O(H_2O), and two N($1\text{-}CH_3im$) coordinate to Mg. The chains are bent about the N of the bridging cyanides at angles of 156.3 (2) and 152.3 (3)°. The bending is attributed to a combination of electronic effects due to back-bonding, electrostatic attraction between the metal centers, and hydrogen bonding. The Fe–N($1\text{-}CH_3im$) bond length [1.950 (2) Å] is shorter than the Fe–NH_3 bond lengths of similar complexes. The imidazole ring coordinated to Fe is staggered with respect to the cis cyanides, but at an angle (ϕ = 34.5°) that is less than the sterically favorable 43.6°. The cyanide trans to the $1\text{-}CH_3im$ ligand on the Fe has a shorter bond length [1.130 (4) Å] than the average cis cyanide bond length of 1.146 Å. The N_3–C_2 bond length is longer for the $1\text{-}CH_3im$ coordinated to Fe than for those of $1\text{-}CH_3im$ coordinated to Mg. The complex has a very large quadrupole splitting (from Mössbauer spectroscopy) of 2.62 ± 0.2 mm/s at 291 K (2.78 mm/s at 77 K). Collectively, our results indicate π bonding between the $1\text{-}CH_3im$ and the low-spin d^5 Fe(III). $1\text{-}CH_3im$ acts as a π *director* to align the electron hole in the dπ Fe orbitals along the Fe–N($1\text{-}CH_3im$) axis. The electron hole primarily occupies a single orbital. The observed π-bonding properties of imidazole have important biological implications.

Introduction

The imidazole (imH, **1**) ring, a five-member nitrogen heterocycle, is an essential component of many biological systems where it occurs in proteins as part of the side chain of the amino acid histidine,[2] in nucleic acid structures as part of the purine ring of adenine and guanine,[3] and in the vitamin B_{12} coenzyme as benzimidazole.[4] In these systems the imidazole functions in a variety of roles; for example, as a proton donor and/or acceptor site for hydrogen bonding, as a specific/general base or nucleophilic catalyst, or as a site for metal ion coordination.[5-9] The imidazole moiety of histidyl residues in a large number of metalloproteins constitutes all or part of the binding sites for various transition-metal ions such as Mn^{2+}, $Fe^{2+,3+}$, $Cu^{+,2+}$, and Zn^{2+}.[8-10] Thus, structural and spectroscopic studies that characterize the bonding between imidazole and transition-metal ions are of considerable importance. Particular attention has been paid to studies of the Fe–imidazole bond because of the role of this bond in the O_2 binding cooperativity mechanism of hemoglobin[11] and in influencing the oxidation–reduction potentials of c-type cytochromes.[12] One approach to the study of Fe–imidazole bonding has been to employ smaller model complexes[9] including a variety of porphyrin complexes[12b] such as the "picket fence" and "pocket" porphyrins[13] among others. An even simpler series of complexes that have also proven useful for evaluating imidazole bonding are complexes of the type $(CN)_5FeL^{3-,2-}$[14-26] and $(NH_3)_5RuL^{2+,3+}$,[27-35] where L

* To whom correspondence should be addressed.
† Present address: Laboratory of Chemical Physics, National Institute of Diabetic and Digestive and Kidney Diseases, National Institute of Health, Bethesda, MD 20892.

(1) A preliminary account of this work was presented at the 43rd Pittsburgh Diffraction Conference, Pittsburgh, PA, Nov 1985.
(2) Creighton, T. E. *Proteins, Structures and Molecular Properties*; W. H. Freeman: New York, 1984; pp 14-16.
(3) Saenger, W. *Principles of Nucleic Acid Structure*; Springer-Verlag: New York, 1984.
(4) Pratt, J. M. *Inorganic Chemistry of Vitamin B_{12}*; Academic Press: New York, 1972.
(5) Barnard, E. A.; Stein, W. D. *Adv. Enzymol.* **1959**, *20*, 51-110.
(6) (a) Walsh, C. *Enzymatic Reaction Mechanisms*; W. H. Freeman: New York, 1979; pp 41-43. (b) Rebek, J., Jr. *Struct. Chem.* **1990**, 129-131. (c) Meot-Ner (Mautner), M. *J. Am. Chem. Soc.* **1988**, *110*, 3075-3080.
(7) Matuszak, C. A.; Matuszak, A. J. *J. Chem. Educ.* **1976**, *53*, 280-284.
(8) Freeman, H. C. *Inorganic Biochemistry*; Eichorn, G. L., Ed.; Elsevier: New York, 1973; Chapter 4, pp 143-152.
(9) Sundberg, R. J.; Martin, R. B. *Chem. Rev.* **1974**, *74*, 471-517.
(10) Sigel, H.; Fischer, B. E.; Prijs, B. *J. Am. Chem. Soc.* **1977**, *99*, 4489-4496. In particular Table VI, p 4494, details the metal binding sites of a number of enzymes and proteins.
(11) (a) Perutz, M. F.; Fermi, G.; Luisi, B.; Shaanan, B.; Liddington, R. C. *Acc. Chem. Res.* **1987**, *20*, 309-321. (b) Suslick, K. S.; Reinert, T. J. *J. Chem. Educ.* **1985**, *62*, 974-983.
(12) Korszun, Z. R.; Moffat, K.; Frank, K.; Cusanovich, M. A. *Biochemistry* **1982**, *21*, 2253-2258.
(13) Collman, J. P.; Brauman, J. I.; Collins, T. J.; Iverson, B. L.; Lang, G.; Pettman, R. B.; Sessler, J. L.; Walters, M. A. *J. Am. Chem. Soc.* **1983**, *105*, 3038-3052. Collman, J. P.; Brauman, J. I.; Iverson, B. L.; Sessler, J. R.; Morris, R. M.; Gibsopn, C. H. *J. Am. Chem. Soc.* **1983**, 3052-3064, for example.
(14) Shepherd, R. E. *J. Am. Chem. Soc.* **1976**, *98*, 3329-3335.

0020-1669/91/1330-2120$02.50/0

is imidazole or a substituted imidazole such as 1-methylimidazole (1-CH_3im, **2**). Despite the interest that has been focused on the $(CN)_5FeL^{3-,2-}$ and $(NH_3)_5RuL^{2+,3+}$ complexes, there have been few structural studies. A complex containing a C-bound isomer of imidazole was reported in 1974.[36] The first crystal structure determination of an N-bound complex, (*l*-histidinato)pentammineruthenium(III) chloride monohydrate, was reported only recently.[37] We now report the first crystal structure of a $(CN)_5FeL^{2-}$ complex, *catena*-$(H_2O)_2$(1-CH_3im)$_2$Mg(μ-CN)-$(CN)_4$(1-CH_3im)$Fe^{III}\cdot H_2O$ (**3**).[38] This low-spin d^5 Fe(III) complex permits an evaluation of the π-bonding ability of imidazole under circumstances that favor such bonding. In addition this complex features Mg–imidazole coordination, which is also of possible importance in biological systems. 1-Methylimidazole is known to have a strong affinity for Mg^{2+}.[39] It has been suggested that Mg^{2+} coordinates to *N*-methylhistidine found in muscle myosin.[40,41] Histidine also represents a possible coordination site in enzymes that require Mg^{2+}.

An evaluation of the π-bonding ability of imidazole is important for understanding the effect of imidazole on the physicochemical properties of hemoproteins and how these properties might be "fine tuned" by changes in Fe–imidazole bond lengths and imidazole orientation or by hydrogen bonding or deprotonation of the pyrrole-like hydrogen (ring position 1). Structural features of **3** strongly indicate π bonding between 1-CH_3im and Fe. Several of these features have not been noted previously and will be useful for future studies of imidazole bonding in biological systems.

Table I. Summary of Crystallographic Data and Data Collection Parameters

formula	$FeMgC_{17}H_{24}N_{11}O_3$
fw	510.60
space group	$P2_1$ (No. 4, unique axis *b*)
cryst system	monoclinic β
a, Å	8.471 (2)
b, Å	15.678 (4)
c, Å	9.722 (2)
α, deg	90
β, deg	112.77 (2)
γ, deg	90
V, Å^3	1190.5 (4)
Z	2
d(calcd), g/cm^3	1.42
d(exptl), g/cm^3	1.39 (flotation, CCl_4/CH_3CN)
cryst dimens, mm	0.25 × 0.25 × 0.325
μ(Mo Kα), cm^{-1}	6.98
radiation	Mo Kα
λ, Å	0.71069
collcn mode	θ/2θ
2θ limits, deg	4.0–55.0
no. of data collcd	2989
no. of unique obsd reflcns >2.5σ	2104
R^a	0.026
$R_w{}^b$	0.029
g	0.001
goodness of fit^c	1.016
max peak in final diff map, e Å^{-3}	0.22
largest shift/esd, final cycle	0.041

$^a R = \sum(|F_o| - |F_c|)/\sum(F_o)$. $^b R_w = \sum(w^{1/2}|F_o - F_c|)/\sum(w^{1/2}F_o)$; $w = (\sigma^2(F) + gF^2)^{-1}$. ^{c}Goodness of fit = $[\sum w(|F_o| - |F_c|)^2/(N_{observns} - N_{params})]^{1/2}$. ^{d}Located near the O(1′) atom.

Experimental Section

Materials. 1-Methylimidazole was obtained from Aldrich and used as received. $Na_3[(CN)_5FeNH_3]\cdot 3H_2O$, the starting material for the preparation of the imidazole complexes, was prepared from sodium nitroprusside (Fisher) by a method described elsewhere.[14,17,42] Reagent grade $MgCl_2$ was used to precipitate the final product. Microanalyses were performed by Galbraith Laboratories, Inc., Knoxville, TN 37921.

Physical Measurements. FTIR spectra were obtained with an IBM IR/32 spectrometer. Samples for IR analyses were powdered and pressed into KBr pellets. Mössbauer spectra were obtained as described elsewhere.[20] The velocity scale was calibrated with a sodium nitroprusside (NP) absorber standard. Line widths for NP were typically 0.27 mm/s. Crystalline samples were ground to a powder before obtaining the Mössbauer spectra. The sample thickness was ~3 mm. Both the source and sample were at room temperature. Low-temperature data were obtained with the sample immersed in liquid N_2. Routine electronic absorption spectra were obtained with an IBM 9420 spectrophotometer.

Crystal Preparation. Solutions of $(CN)_5Fe(1\text{-}CH_3im)^{2-}$ were prepared by a method described previously[17] and precipitated with Mg^{2+} in a manner similar to that described for the Ca^{2+} salts.[22] The complex was obtained by dissolving 2 g (6 mmol) of $Na_3[(CN)_5FeNH_3]\cdot 3H_2O$ and 2.5 g (30 mmol) of 1-methylimidazole in 50 mL of doubly deionized water. The Fe(II) complex, which forms rapidly, was oxidized by the addition of 10 mL of a 3% H_2O_2 solution (12 mmol). The pH of the solution was monitored and maintained between 7 and 8 by the addition of dilute HCl(aq) as required. One hour was allowed for complete oxidation. An equal volume of a nearly saturated solution of $MgCl_2$ (filtered to remove particulates) was added to the reaction mixture, which was then transferred to a porcelin evaporating dish, covered with laboratory tissue, and allowed to evaporate undisturbed at room temperature for several weeks or more. Large crystals of the product were obtained and collected by filtration and washed with diethyl ether. Well-formed red-orange crystals exhibiting tetragonal-bipyramidal morphology were obtained. Anal. Calcd for $C_{17}H_{24}O_3N_{11}FeMg$: C, 39.99; H, 4.74; O, 9.40; N, 30.18; Fe, 10.94; Mg, 4.76. Found: C, 39.98; H, 4.90; O, 8.96;[43]

(15) Bowers, M. L.; Kovacs, D.; Shepherd, R. E. *J. Am. Chem. Soc.* **1977**, *99*, 6555–6561.
(16) Toma, H. E.; Martins, J. M.; Giesbrecht, E. *J. Chem. Soc., Dalton Trans.* **1978**, 1610–1617.
(17) Johnson, C. R.; Shepherd, R. E.; Marr, B.; O'Donnell, S.; Dressick, W. *J. Am. Chem. Soc.* **1980**, *102*, 6227–6235.
(18) Toma, H. E.; Batista, A. A.; Gray, H. B. *J. Am. Chem. Soc.* **1982**, *104*, 7509–7515.
(19) Szecsy, A. P.; Haim, A. *J. Am. Chem. Soc.* **1981**, *103*, 1679–1683.
(20) Johnson, C. R.; Shepherd, R. E. *Inorg. Chem.* **1983**, *22*, 3506–3513.
(21) Johnson, C. R.; Henderson, W. W.; Shepherd, R. E. *Inorg. Chem.* **1984**, *23*, 2754–2763.
(22) Johnson, C. R.; Shepherd, R. E. *Synth. React. Inorg. Met.-Org. Chem.* **1984**, *14*, 339–353.
(23) Warner, L. W.; Hoq, M. F.; Myser, T. K.; Henderson, W. W.; Shepherd, R. E. *Inorg. Chem.* **1986**, *25*, 1911–1914. Shepherd, R. E.; Hoq, M. F.; Hoblack, N.; Johnson, C. R. *Inorg. Chem.* **1984**, *23*, 3249–3252.
(24) Jones, C. M.; Johnson, C. R.; Asher, S. A.; Shepherd, R. E. *J. Am. Chem. Soc.* **1985**, *107*, 3772–3780. Walters, M. A.; Spiro, T. G. *Inorg. Chem.* **1983**, *22*, 4014–4017.
(25) Sabo, E. M.; Shepherd, R. E.; Rau, M. S.; Elliot, M. G. *Inorg. Chem.* **1987**, *26*, 2897–2907.
(26) (a) Eaton, D. R.; Watkins, J. M. *Inorg. Chem.* **1985**, *24*, 1424–1431. (b) Wu, F.-J.; Kurtz, D. M., Jr. *J. Am. Chem. Soc.* **1989**, *111*, 6563–6572.
(27) Sundberg, R. J.; Shepherd, R. E.; Taube, H. *J. Am. Chem. Soc.* **1972**, *94*, 6558–6559.
(28) Sundberg, R. J.; Bryan, R. F.; Taylor, I. F., Jr.; Taube, H. *J. Am. Chem. Soc.* **1974**, *96*, 381–392.
(29) Brown, G. M.; Sutton, J. E.; Taube, H. *J. Am. Chem. Soc.* **1978**, *100*, 2767–2774.
(30) Sundberg, R. J.; Gupta, G. *Bioinorg. Chem.* **1973**, *3*, 39–48.
(31) Tweedle, M. F.; Taube, H. *Inorg. Chem.* **1982**, *21*, 3361–3371.
(32) Isied, S. S.; Kuehn, C. G. *J. Am. Chem. Soc.* **1978**, *100*, 6755–6756.
(33) Hoq, M. F.; Shepherd, R. E. *Inorg. Chem.* **1984**, *23*, 1851–1858.
(34) Elliot, M. G.; Shepherd, R. E. *Inorg. Chem.* **1987**, *26*, 2067–2073.
(35) Krogh-Jespersen, K.; Schugar, M. J. *Inorg. Chem.* **1984**, *23*, 4390–4393.
(36) Imidazoles were found to form carbon-bound complexes (through C-2) with Ru(II). The structure of *trans*-tetraamminecarbonyl(2-(4,5-dimethylimidazoliumyl))ruthenium(II) hexafluorophosphate is reported in ref 27.
(37) Krogh-Jespersen, K.; Westbrook, J. D.; Potenza, J. A.; Schugar, H. J. *J. Am. Chem. Soc.* **1987**, *109*, 7025–7031.
(38) *catena*-diaquabis(1-methylimidazole)magnesium(II)-μ-cyanotetracyano(1-methylimidazole)ferrate(III) monohydrate, *catena*-[Mg-$(H_2O)_2$(1-CH_3im)$_2$(μ-CN)Fe$(CN)_4$(1-CH_3im)]$\cdot H_2O$
(39) (a) Ramirez, F.; Marecek, J. F. *Synthesis* **1979**, 71–74. (b) Sarma, R.; Ramirez, F.; Narayanan, P.; McKeever, B.; Marecek, J. F. *J. Am. Chem. Soc.* **1979**, *101* 5015–5019. (c) Ramirez, F.; Sarma, R.; Chaw, Y. F.; McCaffrey, T.; Marecek, J. F.; McKeever, B.; Nierman, D. *J. Am. Chem. Soc.* **1977**, *99*, 5285–5289. (d) McKee, V.; Ong, C. C.; Redley, G. A. *Inorg. Chem.* **1984**, *23*, 4242–4248.
(40) Ramirez, F.; Shukla, K. K.; Levy, H. M. *J. Theor. Biol.* **1979**, *76*, 351.
(41) Shukla, K. K.; Ramirez, F.; Marecek, J. F.; Levy, H. M. *J. Theor. Biol.* **1979**, *76*, 359.
(42) Brauer, G. *Handbook of Preparative Inorganic Chemistry*, 2nd ed.; Academic Press: New York, 1965; Vol. 2, p 1511.
(43) Galbraith Laboratories, Inc., indicated in their report that the analysis "may not include all of the inorganic oxygen".

N, 29.89; Fe, 10.82; Mg, 4.53. Crystals of **3** are stable for years.

X-ray Structure Determination

(a) Data Collection and Processing. Diffraction measurements of a crystal of compound **3** were carried out on a Nicolet P3 four-circle autodiffractometer system using graphite-monochromated Mo Kα radiation. A summary of the crystallographic data is shown in Table I. The X-ray data were collected from a crystal mounted on a quartz fiber and optically centered on the diffractometer. Rotation and oscillation photographs were taken, and 25 intense reflections were chosen and used for preliminary centering and for determining the orientation matrix and unit cell parameters by least-squares refinement.[44] A preliminary data set was collected and used to identify an independent set of 20 intense reflections ($17.55 \leq \theta \leq 22.28$) for recentering and redetermination of the final unit cell parameters and standard deviations (Table I). The number of formula units per cell, Z, was determined from the measured density. All data were collected at room temperature (18 °C). A quadrant of data was collected (hkl: $+h,+k,+l$, +11,+20,+12) by using a $\theta/2\theta$ scan mode. Several very intense reflections were recollected at a lower tube current and scaled to the rest of the data during data reduction. The intensities of three check reflections were monitored every 100 reflections during the data collection. Although no significant decrease in intensity was observed for these reflections ($\sim$1%), a decay correction was applied. Semiempirical absorption corrections were calculated from a transmission curve based on azimuthal scans of 20 reflections. The program XEMP[45] was used for these corrections (transmission minimum, 0.824; maximum, 0.927). Lorentz and polarization corrections were applied.

(b) Structure Solution and Refinement. The space group, $P2_1$, was chosen on the basis of systematic absences of every second reflection in the $0k0$ series and confirmed by the successful refinement of the structure. The structure was solved by using the heavy-atom method. The positions of the Fe and Mg atoms were determined by analysis of Harker sections. The Fe atom was arbitrarily placed at $y = 0$, defining the origin along the polar screw axis. The remaining non-hydrogen atoms including a water of crystallization were located by using successive difference Fourier syntheses. The water molecule of crystallization was later determined to be disordered, as described below. All non-hydrogen atoms except for the minor site for O(1) were refined by using anisotropic temperature factors. The neutral-atom scattering factors used in the refinement were literature values.[46] Refinement was by blocked-cascade least-squares methods. The function minimized in the least-squares calculation was $\sum w(|F_o| - |F_c|)^2$ with $w = 1/(\sigma^2(F_o) + gF_o^2)$, where σ is the estimated standard deviation based on counting statistics. Weights were based on counting statistics.

Instrumental instabilities were accounted for by modifying the calculated variances for each structure factor by a constant factor of 0.001. Hydrogen atoms were located from Fourier difference maps. Unconstrained refinement of hydrogen atoms leads to several unreasonably short bond lengths.[47] Therefore, the positional coordinates of the imidazole and methyl hydrogen atoms were refined by using a riding model in which the bonding geometry between the hydrogens and the non-hydrogen atoms was constrained to idealized values. The C–H distance was fixed at 0.96 Å. The angles were determined such that the C–H bond had 3-fold symmetry with respect to the hydrogen atoms in the case of the methyl group and a 2-fold axis of symmetry along the C–H bond in the case of the imidazole ring hydrogens. The isotropic temperatures of the hydrogen atoms were allowed to vary independently. The positional parameters for the hydrogen atoms of O(3) were varied independently. Those of O(2) were held fixed in the positions determined from the Fourier difference map. Attempts to refine them diverged, implying that they may actually be disordered. Attempts to refine the peaks found within bonding distance of O(1) as hydrogen atoms resulted in one of the proposed hydrogen atom's temperature factor becoming nonpositive definite. Furthermore, the resulting geometry about the oxygen atom was distorted. An inspection of the U_{eq} for O(1) showed it to be almost twice the average for the rest of the non-hydrogen atoms. From these observations, it was concluded that the water of crystallization was disordered and that one of the putative hydrogen atoms was actually an oxygen atom with an occupancy factor much less than one. The disordered atoms were then refined such that their occupancy factors were held fixed at 0.8 and 0.2 allowing both positional and thermal parameters to vary. The thermal parameters were next held fixed and the occupancy factors allowed to vary with the constraint that the sum of the two factors be unity. This process was iterated over a few cycles until the respective parameters converged. Since the resulting occupancy factors varied only slightly from the original assumption, these values were fixed at the original factors of 0.8 and 0.2 and the refinement completed by using anisotropic thermal parameters for the major site and an isotropic factor for the minor site.

The final agreement factors are in Table I. The positional parameters and isotropic thermal factors of the non-hydrogen atoms are listed in Table II. The positions and thermal parameters of the hydrogen atoms are in Table S1 of the supplementary material. The anisotropic thermal parameters for the non-hydrogen atoms are in Table S2 of the supplementary material. The observed and calculated structure factors are listed in Table S5 of the supplementary material. Estimated standard deviations (esd's) of bond lengths and angles were calculated from the standard errors in the fractional coordinates of the corresponding atomic positions. Esd's are shown in parentheses in all tables.

Table II. Fractional Atomic Coordinates ($\times 10^4$) and Isotropic Thermal Parameters ($Å^2 \times 10^3$) for Non-Hydrogen Atoms of **3**

	x	y	z	U^a
Fe	377 (1)[b]	0	2861 (1)	21 (1)
C(1)	588 (4)	1234 (2)	2848 (3)	38 (1)
N(1)	703 (4)	1953 (2)	2877 (3)	62 (1)
C(2)	2575 (3)	−56 (2)	4485 (2)	26 (1)
N(2)	3816 (3)	−86 (2)	5521 (2)	33 (1)
C(3)	−520 (4)	152 (2)	4400 (3)	31 (1)
N(3)	−950 (4)	241 (2)	5379 (3)	54 (1)
C(4)	1451 (4)	−61 (2)	1414 (2)	28 (1)
N(4)	2124 (4)	−127 (2)	602 (2)	42 (1)
C(5)	−1833 (3)	97 (2)	1227 (2)	26 (1)
N(5)	6897 (3)	118 (2)	10207 (2)	34 (1)
N(6)	140 (3)	−1237 (1)	2881 (2)	26 (1)
C(6)	−634 (4)	−1726 (2)	1689 (3)	33 (1)
C(7)	695 (4)	−1789 (2)	4079 (3)	41 (1)
C(8)	264 (5)	−2597 (2)	3571 (4)	48 (1)
N(7)	−565 (3)	−2546 (2)	2074 (3)	40 (1)
C(9)	−1260 (5)	−3254 (2)	1038 (4)	60 (2)
Mg	5400 (1)	−4 (1)	7852 (1)	25 (1)
N(8)	5259 (3)	−1395 (2)	8095 (3)	37 (1)
C(10)	5351 (5)	−1994 (2)	7196 (4)	44 (1)
C(11)	4638 (6)	−1792 (2)	9048 (4)	54 (2)
C(12)	4371 (6)	−2631 (2)	8675 (5)	65 (2)
N(9)	4811 (4)	−2754 (2)	7498 (3)	46 (1)
C(13)	4739 (7)	−3555 (3)	6676 (6)	79 (2)
N(10)	5443 (3)	1383 (2)	7596 (2)	33 (1)
C(14)	6829 (5)	1898 (2)	8305 (4)	47 (1)
C(15)	6434 (5)	2720 (2)	7909 (4)	54 (2)
C(16)	4232 (5)	1909 (2)	6777 (4)	40 (1)
N(11)	4753 (4)	2721 (2)	6933 (3)	42 (1)
C(17)	3700 (6)	3469 (2)	6229 (5)	69 (2)
O(1)	190 (4)	3518 (2)	1466 (3)	55 (1)
O(1′)	−65 (15)	3657 (7)	1966 (11)	44 (2)[c]
O(2)	3059 (2)	80 (2)	8133 (2)	37 (1)
O(3)	7592 (3)	−146 (2)	7473 (2)	42 (1)

[a] Equivalent isotropic U defined as one-third of the trace of the orthogonalized U_{ij} tensor. [b] Numbers in parentheses are the estimated standard deviations in the least significant digits. See Figure 1 for identity of the atoms. [c] Isotropically refined.

Results and Discussion

Description of the Structure of 3. The molecular structure of **3** is shown in Figure 1 with important bond lengths and bond angles listed in Tables III and IV. The coordination sphere of the Fe(III) consists of five cyanide ligands and 1-CH_3im. Two of the cyanides [CN(5) and CN(2)] act as bridging ligands to the Mg(II) counterions and form continuous chains. The Mg(II) coordination environment is completed by two 1-CH_3im ligands and two water molecules. The asymmetric unit also contains one water of crystallization. The unit cell contents are shown in the stereoview of the crystal packing diagram (Figure 2). As seen in Figure 2, all of the metal–imidazole bonds are approximately parallel to the crystallographic b axis. In particular all of the Fe–imidazole bonds are aligned in the same direction.

(44) All crystallographic calculations were performed on a Data General Eclipse computer using the standard SHELXTL software package by G. M. Sheldrick, Nicolet Instrument Corp., Madison, WI. SHELXTL is part of the Nicolet R3m system.
(45) XEMP is part of the SHELXTL software.
(46) Cromer, D. T.; Waber, J. T. *International Tables for X-ray Crystallography*; Kynoch: Birmingham, England, 1974; Vol. IV. Anomalous-dispersion terms ($\Delta f'$, $\Delta f''$) were included for all atoms with atomic numbers greater than 2.
(47) Churchill, M. R. *Inorg. Chem.* **1973**, *12*, 1213–1214.

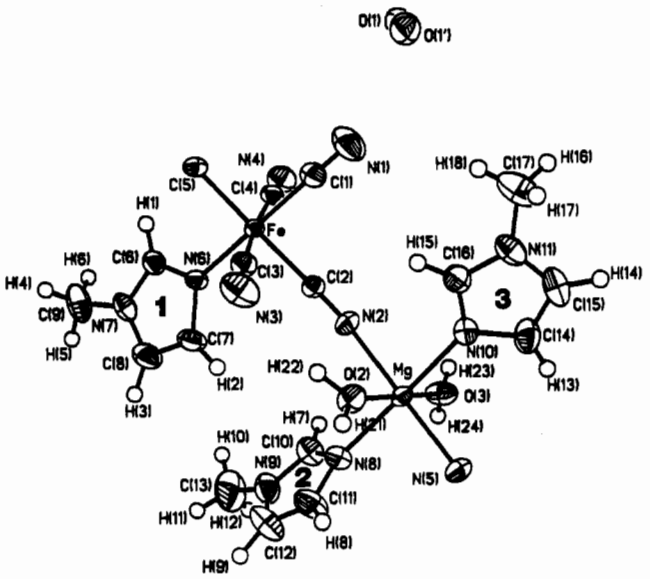

Figure 1. Perspective view and atom-numbering scheme for *catena*-$[Mg(H_2O)_2(1\text{-}CH_3im)_2(\mu\text{-}CN)Fe(CN)_4(1\text{-}CH_3im)]\cdot H_2O$ (**3**). Thermal ellipsoids are drawn at the 50% probability level. Hydrogen atoms are represented by spheres or arbitrary radius. Hydrogen atoms on O(1) are not shown. The numbering for the imidazole rings is also shown.

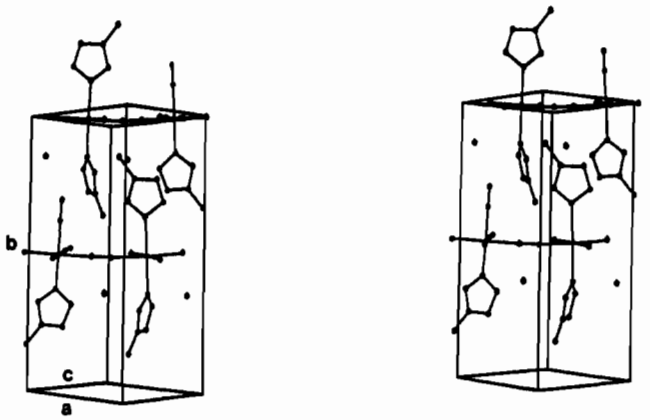

Figure 2. Stereoscopic view of the packing arrangement in unit cells of a crystal of **3**, showing the relationship between chains in the structure. Hydrogen atoms are omitted for clarity. The unconnected atoms are the waters of crystallization.

Table III. Bond Lengths (Å) for **3**

Fe–C(1)	1.943 (3)	C(1)–N(1)	1.130 (4)
Fe–C(2)	1.922 (2)	C(2)–N(2)	1.141 (3)
Fe–C(3)	1.937 (3)	C(3)–N(3)	1.151 (5)
Fe–C(4)	1.951 (3)	C(4)–N(4)	1.143 (4)
Fe–C(5)	1.936 (2)	C(5)–N(5a)	1.147 (3)
Fe–N(6)	1.950 (2)	N(5)–C(5a)	1.147 (3)
Mg–N(2)	2.144 (2)	Mg–N(5)	2.154 (2)
Mg–N(8)	2.202 (3)	Mg–N(10)	2.190 (3)
Mg–O(2)	2.108 (2)	Mg–O(3)	2.040 (3)
	Imidazole 1		
N(6)–C(6)	1.332 (3)	C(7)–C(8)	1.358 (4)
N(6)–C(7)	1.380 (3)	C(8)–N(7)	1.352 (4)
C(6)–N(7)	1.333 (4)	N(7)–C(9)	1.461 (4)
	Imidazole 2		
N(8)–C(10)	1.305 (4)	C(11)–C(12)	1.360 (5)
N(8)–C(11)	1.379 (5)	C(12)–N(9)	1.348 (7)
C(10)–N(9)	1.348 (4)	N(9)–C(13)	1.477 (5)
	Imidazole 3		
N(10)–C(16)	1.318 (4)	C(14)–C(15)	1.349 (5)
N(10)–C(14)	1.371 (4)	C(15)–N(11)	1.372 (4)
C(16)–N(11)	1.336 (4)	N(11)–C(17)	1.472 (5)

The nature of the extended-chain structure is shown more clearly in Figure 3, where a longer portion of the structure is shown

Table IV. Bond Angles (deg) for **3**

	Fe Coordination Environment		
C(1)–Fe–C(2)	89.3 (1)	C(2)–Fe–C(3)	85.2 (1)
C(1)–Fe–C(3)	87.0 (1)	C(2)–Fe–C(4)	90.9 (1)
C(1)–Fe–C(4)	88.5 (1)	C(2)–Fe–C(5)	178.1 (1)
C(1)–Fe–C(5)	88.8 (1)	C(2)–Fe–N(6)	91.0 (1)
C(1)–Fe–N(6)	179.3 (1)	C(3)–Fe–C(4)	174.1 (1)
C(4)–Fe–C(5)	89.1 (1)	C(3)–Fe–C(5)	94.6 (1)
C(4)–Fe–N(6)	92.1 (1)	C(3)–Fe–N(6)	92.4 (1)
C(5)–Fe–N(6)	90.9 (1)	Fe–N(6)–C(7)	129.0 (2)
Fe–C(1)–N(1)	178.0 (3)	Fe–C(4)–N(4)	176.9 (2)
Fe–C(2)–N(2)	174.8 (3)	Fe–C(5)–N(5a)	175.5 (3)
Fe–C(3)–N(3)	175.7 (3)	Fe–N(6)–C(6)	125.6 (2)
	Mg Coordination Environment		
N(2)–Mg–N(5)	177.2 (1)	N(5)–Mg–N(8)	90.4 (1)
N(2)–Mg–N(8)	90.9 (1)	N(5)–Mg–N(10)	90.2 (1)
N(2)–Mg–N(10)	88.3 (1)	N(5)–Mg–O(2)	93.0 (1)
N(2)–Mg–O(2)	84.6 (1)	N(5)–Mg–O(3)	89.9 (1)
N(2)–Mg–O(3)	92.5 (1)	N(8)–Mg–N(10)	178.0 (1)
N(10)–Mg–O(2)	90.7 (1)	N(8)–Mg–O(2)	87.4 (1)
N(10)–Mg–O(3)	91.8 (1)	N(8)–Mg–O(3)	90.1 (1)
O(2)–Mg–O(3)	176.1 (1)	Mg–N(8)–C(10)	128.4 (2)
Mg–C(2)–N(2)	156.3 (2)	Mg–N(8)–C(11)	124.8 (2)
Mg–N(5)–C(5a)	152.3 (3)	Mg–N(10)–C(14)	125.2 (2)
Mg–N(10)–C(16)	130.3 (2)		
	Imidazole 1		
C(6)–N(6)–C(7)	105.3 (2)	C(7)–C(8)–N(7)	106.9 (3)
N(6)–C(6)–N(7)	111.0 (2)	C(6)–N(7)–C(8)	107.9 (2)
N(6)–C(7)–C(8)	108.8 (2)	C(6)–N(7)–C(9)	125.2 (2)
C(8)–N(7)–C(9)	126.8 (3)		
	Imidazole 2		
C(10)–N(8)–C(11)	105.1 (3)	C(11)–C(12)–N(9)	107.0 (4)
N(8)–C(10)–N(9)	112.2 (4)	C(10)–N(9)–C(12)	106.7 (3)
N(8)–C(11)–C(12)	109.0 (4)	C(10)–N(9)–C(13)	125.5 (4)
C(12)–N(9)–C(13)	127.8 (4)		
	Imidazole 3		
C(14)–N(10)–C(16)	104.5 (2)	C(14)–C(15)–N(11)	106.0 (3)
N(10)–C(16)–N(11)	112.5 (3)	C(15)–N(11)–C(16)	106.6 (3)
N(10)–C(14)–C(15)	110.5 (3)	C(16)–N(11)–C(17)	126.3 (3)
C(15)–N(11)–C(17)	127.1 (3)		

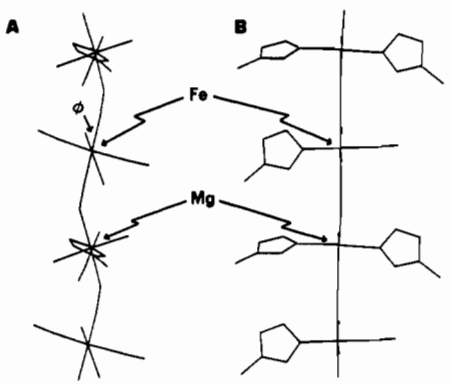

Figure 3. Two schematic views showing the nature of the extended chains in the structure of **3**. View **A** is projected parallel to imidazole 1 and emphasizes the nature of the bent bridges. View **B** is projected approximately normal to the plane of imidazole 1 and emphasizes the relative orientation of the 1-methylimidazoles along the chain. Hydrogen atoms and the waters of crystallization are not shown.

schematically from two views. The bridging angles about N(2) and N(5) are 156.3 (2) and 152.3 (3)°, respectively, leading to the zigzag nature of the chain as shown in Figure 3A. Specific (directed) interactions between the cyanide ligands and the counterions of Fe–cyanide complexes are not unusual[48–50] and

(48) (a) Vannerberg, N.-G. *Acta Chem. Scand.* **1972**, *26*, 2863–2876. (b) Tullberg, A.; Vannerberg, N.-G. *Acta Chem. Scand.* **1971**, *25*, 343–344.
(49) Manoharan, P. T.; Hamilton, W. C. *Inorg. Chem.* **1963**, *2*, 1043–1047.
(50) Wells, A. F. *Structural Inorganic Chemistry*, 5th ed.; Clarendon Press: Oxford, 1984; pp 938–946.

Table V. Distances and Angles for Hydrogen Bonds

D···A	A at	distances, Å		angles, deg	
		D···A	H···A	D–H···A	H–D···A
O(1)···N(1)	x, y, z	2.76			
O(1′)···N(1)	x, y, z	2.81			
O(2)–H(21)···N(4)	$x, y, 1 + z$	2.82	2.14	165.6	10.9
O(3)–H(23)···N(3)	$1 + x, y, z$	2.83	2.09	161.3	13.7
O(3)–H(24)···O(1)	$1 - x, {}^1/_2 + y, 1 - z$	2.74	1.92	167.5	8.8
O(3)–H(24)···O(1′)	$1 - x, -{}^1/_2 + y, 1 - z$	2.71	1.89	167.1	9.0

indeed are expected owing to the lone-pair electrons on the cyanide nitrogens. The extended-chain structure of **3** appears to be unique. A binuclear complex, $[(CN)_5Fe(\mu\text{-}CN)Fe(CN)_4NH_3]^{4-}$, which contains a Fe(III)–CN–Fe(III) bridge has been reported,[51] but the bridge is essentially linear. A nonlinear bridge has been reported[52] for a binuclear Co(III) complex, $[(CN)_5Co(\mu\text{-}CN)Co(NH_3)_5]\cdot H_2O$. Bending of the bridge permits a closer approach of the positive (about Mg) and negative (about Fe) regions of the formula unit. The shortest Fe–C bond is Fe–C(2) [1.922 (2) Å], significantly shorter than Fe–C(5) [1.936 (2) Å], which is the other side of the chain. Likewise, the bridge bond lengths to Mg(II) are unsymmetrical, Mg–N(2) [2.144 (2) Å] and Mg–N(5) [2.154 (2) Å], in such a way as to bring the Mg(II) and Fe(III) closer together about the bridge.

The bridge bends in a direction to bring CN(3) and O(2) closer together. CN(3) and O(2) are also brought closer by distortions in the coordination geometry. The Fe–C(3) bond is tilted toward the bridge [and O(2)] by about 5° compared to the other Fe(III) ligands. The Mg–O(2) bond is tilted toward the bridge [and CN(3)] by about 4–5° compared to the other Mg(II) ligands (see Table IV). The Mg–O(2) bond is also longer than Mg–O(3). A direct hydrogen bond between N(3) and O(2) appears to be unlikely, however, because of the large distance between them (3.445 Å) and the unfavorable angle involved. N(3) and O(2) both participate in hydrogen bonds to an adjacent chain, however, as shown in Table V, and this network of hydrogen bonding may also contribute to the bending.

Back-bonding[53] from Fe(III) into the π^* acceptor orbitals on CN^- may be a factor in producing the bent chain by reducing the C≡N bond order to less than three and introducing some sp^2 hybrid character into the atomic orbitals of the cyanide nitrogen (i.e. an increased contribution from the $:C{=}\ddot{N}:^-$ resonance structure). Back-bonding should also increase the C≡N bond length, however. Except for C(1)–N(1), the average C–N bond length is 1.146 Å. This value appears to be typical.[48-51,54] Molecular orbital studies clearly indicate that some π back-bonding is involved in Fe(III)–CN complexes.[55-57] It seems likely that all three effects—electrostatic attraction, hydrogen bonding, and back-bonding—contribute to the cyanide bridge bending.

Each of the nonbridging cyanides hydrogen bond to water molecules (Table V). CN(1) is hydrogen bonded to the water of crystallization in the same asymmetric unit. O(1) also hydrogen bonds to O(3) on Mg of an adjacent chain, forming a strong link between the chains. Other chains are also linked by hydrogen bonds from CN(3) and CN(4) to Mg-coordinated water molecules.

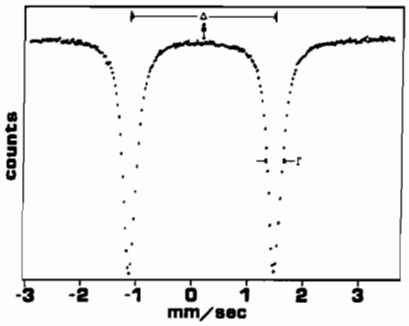

Figure 4. Mössbauer effect spectrum of crystals of **3**.

All three imidazole rings are strictly planar[58] with the sum or internal ring angles equal to 540°, as expected for a planar pentagon. The 1-CH_3 groups deviate significantly (>0.01 Å) out of their respective imidazole ring planes [Table S3 (supplementary material)]. The 1-CH_3 group of imidazole 3 is by 0.04 Å further out of the ring plane than those of imidazoles 1 and 2.

Mg Coordination Environment. The coordination sphere about Mg forms a slightly distorted octahedral geometry. The Mg–O(3) bond distance [2.040 (3) Å] appears to be normal.[59] The Mg–imidazole bonds, Mg–N(8) and Mg–N(10), differ by slightly more than 2.8 σ. Both bond lengths are much longer than previously reported Mg–N(1-CH_3im) bond lengths for Mg(2,4-dinitrophenoxide)$_2$(1-CH_3im)$_2$ [2.115 Å (average)][39b] but are shorter than the value reported for MgTPP(1-CH_3im)$_2$ [2.297 (8) Å].[39d] The imidazole rings form a dihedral angle of 91.5° between them, and each is turned 3–5° from the plane that bisects the planes defined by Mg, O(2), O(3), N(10), N(8), and Mg, N(2), N(5), N(10), N(8).

Fe Coordination Environment. The Fe ligands form a distorted octahedron. Three of the Fe–C bond lengths are the same [1.939 Å (average); Fe–C(1), Fe–C(3), Fe–C(5)]. As discussed above, the Fe–C(2) bond is shorter [1.922 (2) Å] and the Fe–C(4) bond is significantly longer [1.951 (3) Å]. These bond distances are comparable to others that have been reported (see Table VI for some values and Table V of ref 69). The Fe–N(1-CH_3im) bond length [Fe–N(6) = 1.950 (2) Å] is significantly shorter than the Fe–NH_3 bond lengths of $(CN)_5Fe(NH_3)^{2-}$ [2.015 (13) Å] and $(CN)_5Fe(\mu\text{-}CN)Fe(CN)_4(NH_3)^{4-}$ [2.08 (4) Å] (Table VI). Part of this bond length decrease results from iron–ligand π interactions.

Three main factors affect the strength of metal–ligand π interactions:[70-72] (1) the relative energies of the metal and ligand orbitals, (2) the spatial overlap between these orbitals, and (3) the metal electronic configuration. A ligand is a potential π donor if it has occupied π orbital(s) (HOMO) at high energy with large

(51) Roder, P.; Ludi, A.; Chapuis, G.; Schenk, K. J.; Schwarzenbach, D.; Hodgson, K. O. *Inorg. Chim. Acta* **1979**, *34*, 113–117.
(52) Both the μ-isocyano and μ-cyano isomers have been studied, and each has the nonlinear bridge structure: (a) Fronczek, F. R.; Schaefer, W. P. *Inorg. Chem.* **1974**, *13*, 727–732. (b) Wang, B.-C.; Schaefer, W. P.; Marsh, R. E. *Inorg. Chem.* **1971**, *10*, 1492–1497.
(53) A clarification of terms used in this paper is warranted. π bonding refers specifically to the transfer of π-electron density from ligand to metal (sometimes called forward donation), and (π) back-bonding or back-donation refers (as usual) to π-electron-density transfer from metal to ligand.
(54) (a) Sharpe, A. G. *The Chemistry of Cyano Complexes of the Transition Metals*; Academic Press: New York, 1976. (b) Britton, D. *Perspect. Struct. Chem.* **1967**, *1*, 109.
(55) Shulman, R. G.; Sugano, S. *J. Chem. Phys.* **1965**, *42*, 39–43.
(56) Alexander, J. J.; Gray, H. B. *J. Am. Chem. Soc.* **1968**, *90*, 4260–4271.
(57) Calabrese, A.; Hayes, R. G. *J. Am. Chem. Soc.* **1974**, *96*, 5034–5062.
(58) Tables of least-squares best planes and the dihedral angles between them can be found in the supplementary material (Tables S3 and S4).
(59) Sarma, R.; Ramirez, F.; McKeever, B.; Chan, Y. F.; Marecek, J. F.; Nierman, D.; McCaffrey, T. M. *J. Am. Chem. Soc.* **1977**, *99*, 5289–5295. Narayanan, P.; Ramirez, F.; McCaffrey, J.; Chan, Y. F.; Marecek, J. F. *J. Org. Chem.* **1978**, *43*, 24.
(60) Tullberg, A.; Vannerberg, N.-G. *Acta Chem. Scand.* **1974**, *A28*, 340–346.
(61) Swanson, B. I.; Hamburg, S. I.; Ryan, R. R. *Inorg. Chem.* **1974**, *13*, 1685–1687.
(62) Schaefer, W. P. *Inorg. Chem.* **1987**, *26*, 1820–1821. Henderson, W. W.; Shepherd, R. E.; Abola, J. *Inorg. Chem.* **1986**, *25*, 3157–3163.
(63) Keppler, B. K.; Wehe, D.; Endres, H.; Rupp, W. *Inorg. Chem.* **1987**, *26*, 844–846.
(64) Wishart, J. F.; Bino, A.; Taube, H. *Inorg. Chem.* **1986**, *25*, 3318–3321.
(65) Collins, D. M.; Countryman, R.; Hoard, J. L. *J. Am. Chem. Soc.* **1972**, *94*, 2066–2072.
(66) Scheidt, W. R.; Osvath, S. R.; Lee, Y. J. *J. Am. Chem. Soc.* **1987**, *109*, 1958–1963.
(67) Little, R. G.; Dymock, K. R.; Ibers, J. A. *J. Am. Chem. Soc.* **1975**, *97*, 4532–4539.
(68) Scheidt, W. R.; Lee, Y. J.; Luangdilok, W.; Haller, K. J.; Anzai, K.; Hatano, K. *Inorg. Chem.* **1983**, *22*, 1516–1522.
(69) Scheidt, W. R.; Haller, K. J.; Hatano, K. *J. Am. Chem. Soc.* **1980**, *102*, 3017–3021.
(70) Johnson, C. R. Ph.D. Dissertation, University of Pittsburgh, 1983.
(71) Lay, P. A. *Inorg. Chem.* **1984**, *23*, 4775–4777.
(72) Johnson, C. R.; Shepherd, R. E. *Inorg. Chem.* **1983**, *22*, 2439–2444.

Table VI. Bond Length Data for Related Structures

metal complex[a]	M–N(heterocycle), Å	M–X(trans), Å	M–X(cis), Å	φ,[b] deg	ref
$(CN)_5Fe(1\text{-}CH_3im)^{2-}$	1.950 (2)	Fe–C, 1.943 (3)	Fe–C, 1.922 (2), 1.937 (3), 1.951 (3), 1.936 (2)	34.5 (89.0)	this work
$(CN)_5Fe(NH_3)^{2-}$	2.015 (13)[c]	Fe–C, 1.891 (11)	Fe–C, 1.932 (8), 1.945 (8)[g]		60
$(CN)_5Fe\text{–}NC\text{–}Fe(CN)_4(NH_3)^{4-}$	2.08 (4)[c]	Fe–C, 1.85 (6)			51
$Fe(CN)_6^{3-}$		Fe–C, 1.927 (14), 1.952 (16), 1.971 (19)[g]			48a
$Fe(CN)_6^{4-}$		Fe–C, 1.900 (7)			61
$(NH_3)_5Co(5\text{-}CH_3imH)^{3+}$	1.941 (5)	Co–N, 1.966 (5)	Co–N, 1.969 (3), 1.964 (4)[g]	*d*	62
$(NH_3)_5Ru(his)^{3+}$	2.020 (8)	Ru–N, 2.111 (9)	Ru–N, 2.07 (1), 2.07 (1), 2.12 (1), 207 (1)	*e*	37
$(Cl)_5Ru(imH)^{2-}$	2.044 (12)	Ru–Cl, 2.446 (4)	Ru–Cl, 2.378 (3), 2.364 (3)[g]	*d*	63
$(NH_3)_5Ru(CH_3pz)^{4-}$	2.08 (1)	Ru–N, 2.10 (1)	Ru–N, 2.118 (8), 2.107 (9), 2.112 (9), 2.109 (9)	43.4 (92.4)	64
$(NH_3)_5Ru(CH_3pz)^{3-}$	1.95 (1)	Ru–N, 2.17 (1)	Ru–N, 2.122 (7), 2.138 (8)[g]	*d*	64
$Fe(TPP)(imH)_2^{+}$	1.957 (4)			39	
	1.991 (5)			18	65
$Fe(TPP)(imH)_2^{+}$	1.977 (3)			5.7	
	1.964 (3)			41.4	66
$Fe(PPIX)(1\text{-}CH_3im)_2$	1.966 (5)			16	
	1.988 (5)			3	67
Fe(TPP)(CN)(py)	2.075 (3)	Fe–C, 1.908 (4)		*f*	68
$Fe(TPP)(CN)_2^{-}$		Fe–C, 1.975 (2)			69

[a] Abbreviations: 1-CH_3im, 1-methylimidazole; 5-CH_3imH, 5(4)-methylimidazole; his, *l*-histidine; imH, imidazole; CH_3pz^+, *N*-methylpyrazinium ion; TPP, dianion of *meso*-tetraphenylporphyrin; PPIX, dianion of protoporphyrin IX. See the original references for counterions and complete formula. [b] The value in parenthesis is the dihedral angle between the *yz* and *xz* planes as defined in Figure 6. [c] Fe–NH_3 bond length. [d] A bisecting angle is required by symmetry. [e] Stated to be bisecting. [f] Not reported but shown as staggered in figure. [g] The remaining bond lengths are symmetry related.

radial extension. Imidazole and its methylated derivatives have three filled orbitals at relatively high energies, which are well separated from the lower core orbitals.[73-75] The HOMO, π_1, has electron density based primarily on the carbon atoms of the imidazole ring. The next highest orbital, π_2, has electron density based primarily on the nitrogen atoms. The third orbital, with energy close to π_2, is an n orbital consisting of the lone pair on the pyridine-like nitrogen (position 3).

UV–visible electronic and Mössbauer studies indicate that the π_1 and π_2 orbitals are of high enough energy and of sufficient spatial extent to overlap with the Fe(III) dπ orbitals.[70] The visible absorption spectra of $(CN)_5FeL^{2-}$ complexes show two characteristic bands that have been assigned as ligand-to-metal charge-transfer (LMCT) transitions[21,24] in part on the basis of correlations among the electronic absorption spectral data for $(CN)_5FeL^{2-}$ complexes. $(NH_3)_5RuL^{3+}$ complexes,[21,28,35] and CuL_4^{2+} complexes.[75-77] The assignment of these LMCT transitions as $d\pi \leftarrow \pi_1$ and $d\pi \leftarrow \pi_2$[21] was confirmed by resonance Raman studies.[24]

The room-temperature Mössbauer spectrum of powdered crystals of **3** shown in Figure 4 displays a well-developed, sharp, symmetrical doublet with a center shift, δ, vs NP of 0.16 ± 0.02 mm/s. This value, which is typical of low-spin Fe(III) complexes, is not very sensitive to the ligand environment.[20,78] The quadrupole splitting, Δ, is 2.62 ± 0.02 mm/s at 291 K (2.78 ± 0.04 mm/s at 77 K). As has been demonstrated for a series of $(CN)_5FeA^{2-}$ salts (A = nitrogen heterocycle), Δ is very sensitive to the nature of A.[20] For π-acceptor ligands Δ depends upon the ligand's conjugate acid pK_a. Complexes that exhibit LMCT transitions in the visible region (A = imidazoles, pyrazoles, 4-aminopyridine, and 4-dimethylaminopyridine) have large quadrupole splittings (~2.5 mm/s) that are nearly independent of pK_a. The quadrupole splitting for **3** is the largest reported for any $(CN)_5FeA^{2-}$ complex, exceeding the values for the Ca^{2+} and Zn^{2+} salts reported previously.[20]

As a class, ligands which form complexes with $(CN)_5Fe^{2-}$ that have low-energy LMCT transitions and large quadrupole splittings must be considered potential π donors. It is difficult, however, to evaluate π-donor/π-acceptor ability quantitatively. Even classic π-interacting ligands such as CO are still under evaluation.[79,80] Crystal structure data can be used to evaluate π bonding. Hambley and Lay compared the π-bonding ability of Cl^- in an isomorphous series of $[(NH_3)_5MCl]Cl_2$ compounds (M = Cr, Co, Rh, Ir, Ru, Os) using structural data.[81] We identify the following structural features to indicate π bonding between L and M: (1) a short M–L bond length; (2) a nonstaggered (partially eclipsed) orientation of L; (3) a structural influence on the ligand trans to L; (4) internal bond length changes of L. Each of these features is discussed below.

Hambley and Lay gave convincing evidence for π bonding of Cl^- in d^5 and d^3 complexes by showing that M–Cl bond length is shorter for these complexes than it would be in the absence of π bonding by using M–NH_3 bond lengths as an internal standard.[81] A direct comparison between imidazole and ammonia Fe–N bond lengths is not useful, however, because imidazole and ammonia are substantially different ligands. Ammonia is about 100 times stronger as a σ base (for protons) than imidazole. This would suggest an inherently shorter Fe–N(ammonia) bond length. This is not the case, however, owing to the difference in hybridization of the coordinating nitrogen (sp^3 for NH_3 and sp^2 for imidazole). M–N bond lengths are always shorter for imidazole than ammonia for this reason. We can compare cases where imidazole π bonding is or is not important. A Co(III) complex, $(NH_3)_5Co(5\text{-}CH_3imH)^{3+}$, is a case where π donation is not important.[62] A low-spin d^6 ion such as Co(III) has no empty π orbitals at low energy and cannot be an effective π acceptor. The C–N(imidazole) bond length is ~0.025 Å or 1.3% shorter than the Co–NH_3 bond length (refer to Table VI). For $(NH_3)_5Ru(his)^{3+}$, where π bonding is possible, the Ru–N(imidazole) bond length is ~0.070 Å or 3.3% shorter than the Ru–NH_3 (2.09 Å average) bond length.[37]

The comparison cannot be made within a single complex for Fe(III). With 2.02 Å used as an estimate for the Fe–NH_3 bond length, the Fe–N(imidazole) bond length is ~0.07 Å or 3.5% shorter than the Fe–NH_3 bond length. Unfortunately, the esd's for the two known Fe–NH_3 bond lengths [2.015 (13) and 2.08 (4) Å][51,60] are large, making this estimate tentative. We have used the smaller bond length to make our estimate conservative.

(73) DelBene, J.; Jaffe, H. H. *J. Chem. Phys.* **1968**, *48*, 4050–4055. Sundbom, M. *Acta Chem. Scand.* **1971**, *25*, 487–511. Ha, T. K. *J. Mol. Struct.* **1979**, *51*, 87–98.
(74) Craddock, S.; Findlay, R. H.; Palmer, M. H. *Tetrahedron* **1973**, *29*, 2173–2181.
(75) Bernarducci, E.; Bharadwaj, P. K.; Krogh-Jespersen, K.; Potenza, J. A.; Schugar, H. J. *J. Am. Chem. Soc.* **1983**, *105*, 3866–3875.
(76) Fawcett, T. G.; Bernarducci, E. E.; Krogh-Jespersen, K.; Schugar, H. J. *J. Am. Chem. Soc.* **1980**, *102*, 2598–2604.
(77) Bernarducci, E.; Schwindinger, W. F.; Hughey, J. R., IV; Krogh-Jespersen, K.; Schugar, H. J. *J. Am. Chem. Soc.* **1981**, *103*, 1686–1691.
(78) Golding, R. M. *Applied Wave Mechanics*; Van Nostrand: New York, 1969; Chapter 9.
(79) Zink, J. I.; Chang, T.-H. *J. Am. Chem. Soc.* **1987**, *109*, 692–698.
(80) Shepherd, R. E.; Proctor, A.; Henderson, W. W.; Myser, T. K. *Inorg. Chem.* **1987**, *26*, 2440–2444.
(81) Hambley, T. W.; Lay, P. A. *Inorg. Chem.* **1986**, *25*, 4553–4558.

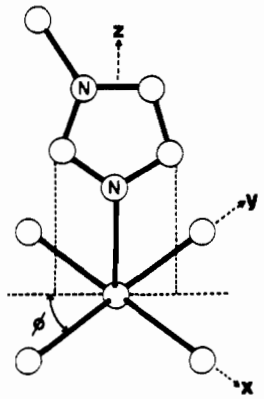

Figure 5. Schematic diagram illustrating the definition of the angle ϕ and the coordinate axis system used in discussions of the bonding about the Fe center, adapted from a similar figure in ref 85.

Low-spin Fe(III) and Ru(III), unlike Co(III), can act to accept π-electron density from a donor ligand. Whereas a M–N(imidazole) bond might be expected to be ~1.3% shorter than a M–NH_3 bond when only σ bonding is important, the bond is ~3% shorter when M = Ru(III) or Fe(III). This is indicative of a π-bonding interaction between imidazole and these low-spin d^5 ions.

When imidazole is forced to compete with other known π-donor ligands [such as Cl^- in $(Cl)_5Ru(imH)^{2-}$], the Ru–N(imidazole) bond length is longer [2.044 (12) Å][63] than with other ligands that cannot π donate: $(NH_3)_5Ru(his)^{3+}$ [2.020 (8) Å].[37] The Fe–N(imidazole) bond length [1.950 (2) Å] is much shorter than a reported Fe–N(pyridine) bond length [2.075 (3) Å].[68] In contrast to the π-donor properties of imidazole, pyridine is known to be a weak π acceptor.[72,82] Imidazole is an electron-donating ligand in both the σ and π sense—much more electron donating than other nitrogen heterocycles except those with very strongly electron-releasing substituents (e.g. $-NH_2$).

For comparison, Table VI displays structural data for a representative strong π-acceptor ligand. When *N*-methylpyrazinium, CH_3pz^+, coordinates to Ru(III), the Ru–N(CH_3pz^+) bond length is ~1.4% shorter than the average Ru(III)–NH_3 bond length.[64] When coordinated to Ru(II), a classic π-back-donating metal ion,[83,84] the Ru–N(CH_3pz^+) bond length is ~8.8% shorter than the average Ru(II)–NH_3 bond length.[64] This observation is consistent with a considerable amount of back-bonding from Ru(II) to CH_3pz^+.[64] Conversely, the ~3% shorter M–N(imidazole) bond length compared to the M–NH_3 bond length for M = Ru(III) and Fe(III) is indicative of π bonding from imidazole to the metal ion. It has been noted[71] that π back-bonding is more favorable than is π bonding because the orbital overlap is inherently greater for interactions between the metal orbitals and ligand π^* orbitals than between the ligand π orbitals and metal orbitals.

The orientation of the imidazole ligand is also influenced by π bonding. The factors specifying the preferred orientation of imidazole ligands in metalloporphyrins have been discussed recently.[85] Figure 5 shows the local axis system and defines the dihedral angle ϕ, which describes the imidazole ring orientation relative to the *yz* plane.[65,85] A value of $\phi = 0°$ corresponds to an eclipsed conformation, and a value of $\phi \approx 45°$ corresponds to a staggered conformation with respect to the cis ligands. For **3** the value of ϕ for imidazole 1 is 34.5°. 1-CH_3im (imidazole 1) is rotated from the eclipsed conformation toward the bridging cyanides [CN(2) and CN(5)] and toward imidazole 2 on Mg.

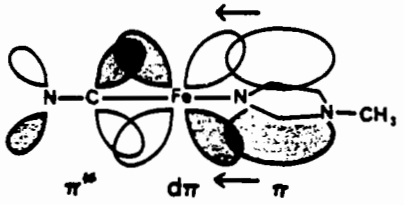

Figure 6. Illustration of the orbital interactions that permit π donation from imidazole through Fe to the trans cyanide, adapted from a similar figure in ref 87.

Nonbonded intramolecular interactions (crystal packing effects) may affect the imidazole 1 orientation, but it seems unlikely that such effects would favor more steric interaction between imidazoles 1 and 2. In fact, structural features at imidazole 2 seem to accommodate this interaction. The imidazole 2 ring plane is tilted 12° from the normal to the plane defined by Mg, N(2), N(5), O(2), O(3) and rotated ~3° from the angle that bisects the planes defined by Mg, N(8), N(10), N(2), N(5), and Mg, N(8), N(10), O(2), O(3). (The imidazole 3 ring plane is not tilted but is rotated ~5° from the bisecting angle in the same sense as imidazole 2 such that both imidazole planes remain nearly orthogonal and imidazole electron–electron repulsion is minimized.)

Imidazole 1 also interacts with imidazole 3 on the adjacent chain (see Figure 2), but it is unclear why the Mg-bound imidazole 3 would remain in a nearly staggered conformation while the Fe bound imidazole 1 turns 9° from the staggered conformation. Neither imidazole 1 nor imidazole 3 is tilted. The principle factors influencing the imidazole 1 orientation seem to derive from the Fe center itself. For porphyrin complexes electronic effects (π bonding) favor $\phi = 0°$ to maximize the π interaction between imidazole and the metal.[85] There is a tendency toward small ϕ values for a wide variety of porphyrin complexes with various metal ions in a variety of oxidation and spin states.[85] Theoretical calculations indicate that the principle interaction explaining the sterically unfavorable angles is an imidazole pπ–metal pπ interaction with metal dπ orbitals participating to only a small extent. The low-spin Fe(III) system (the only low-spin d^5 case considered) was found to be unique, however, in that imH pπ–Fe dπ interactions are important and vary with ϕ. It should be emphasized that the electronic effects that favor $\phi = 0°$ are only important when strongly π-interacting ligands are in the positions cis to the imidazole—such as a porphyrin ring or cyanides. If the cis ligands are non-π bonding (such as ammonia) and exert no influence upon the metal dπ orbitals, imidazole can effectively overlap the metal orbitals even at $\phi = 45°$. The nitrogen heterocycle in $(NH_3)_5MA$ complexes is invariably in a staggered conformation ($\phi \approx 45°$) even for cases where π bonding or π back-bonding is known to be significant, for example, in $(NH_3)_5Ru(CH_3pz)^{3+}$[64] and $(NH_3)_5Ru(pyrazine)^{2+}$.[86] The ϕ value of 34.5° in complex **3** is consistent with the influence of π bonding upon this angle.

Structural data for several low-spin Fe(III) porphyrin complexes are given in Table VI. A variety of data at different ϕ angles are available. The Fe–N(imidazole) bond length is always longer for the smaller ϕ values.[85] The Fe–N(imidazole) bond lengths at larger ϕ values [$\phi = 39°$, 1.957 (4) Å; $\phi = 41.4°$, 1.964 (3) Å; $\phi = 16°$, 1.966 (5) Å] are all essentially identical with the Fe–N(imidazole) bond length of **3** [$\phi = 34.5°$, 1.950 (2) Å].

Further evidence for imidazole π bonding derives from an examination of the structural trans influence of this ligand. A conventional view of the trans influence by π donation from imidazole is shown in Figure 6. The donation of π-electron density from the π_1 or π_2 orbitals of imidazole into the partially filled (or empty) dπ orbitals of Fe (or other metal) transfers electron density to the trans ligand. If the trans ligand is a π acceptor, the electron density can "flow" into the π^* orbital, reinforcing the π back-bonding interaction with this ligand. If the trans ligand is another

(82) Pyridine does not have a high-energy HOMO as does imidazole or a LUMO as low in energy as does pyrazine, a good π acceptor.
(83) Taube, H. *Survey of Progress in Chemistry*; Scott, A. F., Ed.; Academic Press: New York, 1973; Vol. 6, Chapter 1.
(84) Ford, P.; Rudd, De F. P.; Gaunder, R.; Taube, H. *J. Am. Chem. Soc.* **1968**, *90*, 1187–1194.
(85) Scheidt, W. R.; Chipman, D. M. *J. Am. Chem. Soc.* **1986**, *108*, 1163–1167.
(86) Greso, M. E.; Creutz, C.; Quicksall, C. O. *Inorg. Chem.* **1981**, *20*, 1522–1528.

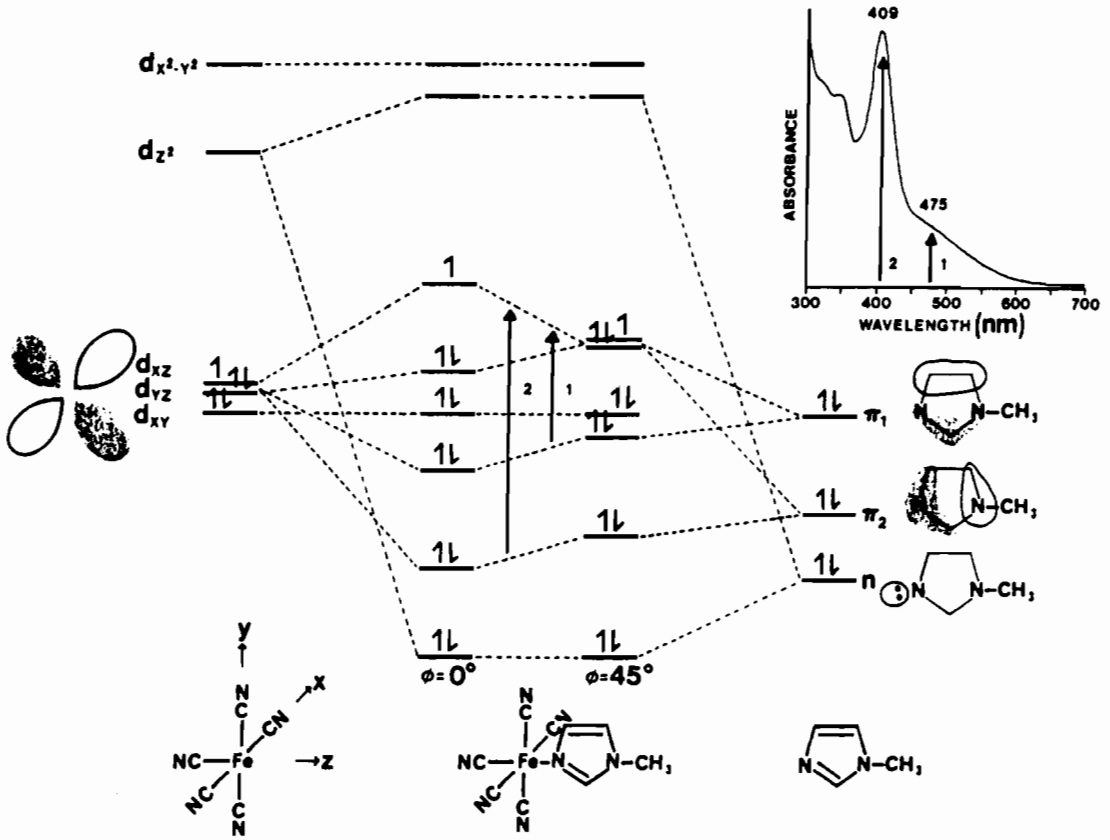

Figure 7. Qualitative molecular orbital diagram for $(CN)_5Fe(1\text{-}CH_3im)^{2-}$. The electronic absorption spectrum of $(CN)_5Fe(1\text{-}CH_3im)^{2-}$ is shown in the upper right-hand corner.

π donor, the π interaction is repulsive and should cause an increase in the bond lengths of both M–N(imidazole) and M–L(trans). This effect is seen in $(Cl)_5Ru(imH)^{2-}$, where Ru–Cl(trans) is longer than Ru–Cl(cis) (see Table VI) and Ru–N(imidazole) is longer than in $(NH_3)_5Ru(his)^{3+}$. In **3** the Fe–C(trans) bond length is neither the shortest nor longest Fe–C bond in the complex so no trans influence is clearly evident from this bond length. The trans cyanide length, C(1)–N(1), is the shortest in the structure. This contradicts the expectation that the trans cyanide bond would lengthen if imidazole is a π donor and electron density transfers to CN^- π^* orbitals.

The Figure 7 qualitative molecular orbital diagram for $(CN)_5Fe(1\text{-}CH_3im)^{2-}$ resolves this discrepancy. The imidazole n (lone-pair) orbital forms a strong σ bond with the Fe d_{z^2} orbital. The imidazole π_1 and π_2 orbitals interact with the Fe d_{xz} and d_{yz} orbitals. The $d_{x^2-y^2}$ and d_{xy} orbitals are non-bonding toward the imidazole. The π_1 and π_2 orbitals shown in the figure are based on calculations for imidazole[73] and should approximate those of 1-methylimidazole. Better overlap should occur between π_2 and the $d\pi$ orbitals because π_2 has significantly more electron density at N(6) (ring position 3) than does π_1. This is consistent with the relative intensities of the LMCT transitions shown in the absorption spectrum in the upper right-hand corner of the figure. LMCT transitions 1 at 475 nm and 2 at 409 nm are assigned to $d\pi \leftarrow \pi_1$ and $d\pi \leftarrow \pi_2$ orbital excitations as shown by the vertical lines on the energy level diagram.

The energy of these transitions should depend upon the value of ϕ. At $\phi = 45°$ the imidazole π orbitals interact equally with d_{yz} and d_{xz} and these orbitals will be degenerate [electronic configuration $d_{xy}^2(d_{yz},d_{xz})^3$], if the $(CN)_5Fe$ fragment is itself not distorted from C_{4v} symmetry. A static Jahn–Teller distortion to rhombic symmetry along the long Fe–C(4) bond, for example, also removes the degeneracy. At $\phi = 0°$ the imidazole π orbitals interact more strongly with the d_{xz} orbital—the orbital perpendicular to the imidazole plane.

At $\phi = 45°$ the electron hole is distributed over the d_{xz} and d_{yz} orbitals (and to a lesser extent the d_{xy} orbital because the energy differences are very small and extensive mixing can occur through spin–orbit coupling). At $\phi = 0°$ the electron hole is nearly exclusively located in the d_{xz} orbital (electronic configuration $d_{xy}^2d_{yz}^2d_{xz}$). A half-occupied $d\pi$ orbital tends to interact with the π-donor ligand (imidazole), while the fully occupied $d\pi$ orbitals tend to interact with the π-acceptor ligands (CN^-).[88,89] The d-orbital vacancy is oriented to overlap favorably with the imidazole π system. At intermediate ϕ values the hole is unequally distributed between the d_{xy} and d_{yz} orbitals. At $\phi = 34.5°$ for **3** the d_{xz} and d_{yz} orbitals will be split only slightly by the imidazole orbitals. The orbitals are split further by rhombic distortion of the cyanide ligands—the Fe–C(2) bond is shorter and the Fe–C(4) bond is longer than the other Fe–C bonds. *The net result of the preference for the hole to reside in d_{xz} (and d_{yz}) is to reduce the electron density available for back-bonding from Fe to the cyanides particularly along the z axis where a single cyanide must compete for π-electron density.* The large quadrupole splitting indicates a nonspherical electron hole distribution and is consistent with the hole residing primarily in a single orbital. Rather than receiving more electron density from the imidazole, the trans cyanide receives *less*. The bond length of the trans cyanide is shortened indicating less π back-bonding to this cyanide compared to the cis cyanides. In terms of a trans influence the imidazole is better described as a π *director* than a π donor. Imidazole is a π director in the sense that the imidazole determines the axis along which the hole is aligned.

When the C(1)–N(1) bond length becomes shorter, the Fe–C(1) bond length is expected to lengthen compared to the other Fe–C bonds. This is not observed. The σ component of the Fe–C bond must also be considered. Cyanide is a very strong σ donor and is expected to be a better σ base than imidazole (HCN, pK_a = 9; imH_2^+, pK_a = 7). There should be less σ electron density along

(87) Chang, C. K.; Traylor, T. G. *J. Am. Chem. Soc.* **1973**, *95*, 8477–8479.
(88) Sakaki, S.; Yanase, Y.; Hagiwara, N.; Takeshita, T.; Naganuma, H.; Ohyoshi, A.; Ohkubo, K. *J. Phys. Chem.* **1982**, *86*, 1038–1043.
(89) Byrn, M. P.; Katz, B. A.; Keder, N. L.; Levan, K. R.; Magurany, C. J.; Miller, K. M.; Pritt, J. W.; Strouse, C. E. *J. Am. Chem. Soc.* **1983**, *105*, 4916–4922.

Table VII. Comparison of Bond Length Data for 1-Methylimidazole

complex[a]	bond length, Å						ref
	N_3–C_2	N_3–C_4	C_4–C_5	C_5–N_1	N_1–C_2	N_1–CH_3	
			π-bonding				
$(CN)_5Fe(1\text{-}CH_3im)^{2-}$ (**3**)	1.332 (3)	1.380 (3)	1.358 (4)	1.352 (4)	1.333 (4)	1.461 (4)	*b*
$Fe(PPIX)(1\text{-}CH_3im)_2$ (**4**)	1.330 (8)	1.368 (8)	1.347 (8)	1.355 (8)	1.329 (7)	1.461 (7)	67
	1.322 (7)	1.369 (9)	1.347 (9)	1.352 (10)	1.348 (8)	1.471 (8)	
av	1.328						
			non-π-bonding				
$Mg(H_2O)_2(1\text{-}CH_3im)_2^{2+}$ (**3**)	1.305 (4)	1.379 (5)	1.360 (4)	1.348 (7)	1.348 (4)	1.477 (5)	*b*
	1.318 (4)	1.371 (4)	1.349 (5)	1.372 (4)	1.336 (4)	1.472 (5)	
$Mg(TPP)(1\text{-}CH_3im)_2$[c] (**5**)	1.314 (13)	1.373 (14)	1.324 (15)	1.282 (15)	1.399 (14)	1.410 (16)	39d
$Mn(TPP)(1\text{-}CH_3im)$ (**6**)	1.295 (4)	1.378 (4)	1.338 (5)	1.326 (4)	1.348 (4)	1.492 (5)	96
$Fe(TPP)(NO)(1\text{-}CH_3im)$ (**7**)	1.304 (6)	1.389 (7)	1.324 (9)	1.352 (8)	1.328 (8)	1.498 (8)	93
$Co(TPP)(1\text{-}CH_3im)$ (**8**)	1.316 (6)	1.377 (5)	1.355 (7)	1.371 (6)	1.365 (6)	1.491 (6)	97
av	1.309						
overall av		1.376	1.347	1.354	1.342	1.478	
$Fe(Piv_2C_8)(1\text{-}CH_3im)$ (**9**)	1.35 (4)	1.25 (3)	1.24 (4)	1.34 (4)	1.45 (4)	1.53 (5)	98
$Fe(T_{piv}PP)(O_2)(1\text{-}CH_3im)$ (**10**)	1.41 (2)	1.41 (2)	1.29 (3)	*d*	*d*	1.36 (3)	94
$Co(OEP)(1\text{-}CH_3im)$ (**11**)	1.30 (2)	1.42 (2)	1.37 (2)	*e*	1.36 (2)	1.52 (2)	99

[a] Abbreviations: $1\text{-}CH_3im$, 1-methylimidazole; PPIX, dianion of protoporphyrin IX; TPP, dianion of *meso*-tetraphenylporphyrin; Piv_2C_8, dianion of $\alpha,\alpha,5,15$-[2,2′-(octanediamido)diphenyl]-$\alpha,\alpha,10,20$-bis(*o*-pivalamidophenyl)porphyrin; $T_{piv}PP$, dianion of *meso*-$\alpha,\alpha,\alpha,\alpha$-tetrakis(*o*-pivalamidophenyl)porphyrin; OEP, dianion of octaethylporphyrin. [b] This work. [c] The second $1\text{-}CH_3im$ is symmetry related to the first. [d] the $1\text{-}CH_3im$ is disordered between two symmetry-related sites. N_3 sits on a 2-fold axis. [e] Not reported.

the *z* axis (one CN^- and one imidazole) than along the x and y axis (two CN^- groups each). This allows CN(1) to form a stronger (shorter) bond to the Fe than expected on the basis of the C(1)–N(1) bond length while not receiving compensatory π-back-bonding electron density because of the $d\pi$ hole alignment. For comparison, $(CN)_5Fe(NH_3)^{2-}$ shows a more typical behavior. Ammonia is not a π donor (director), and the electron hole will not be strongly aligned along the particular axis in $(CN)_5Fe(NH_3)^{2-}$ ($Na_2[(CN)_5FeNH_3]$, Δ = 1.78 mm/s at 80 K; see ref 20). Approximately equal amounts of π-electron density should be available along each axis for back-bonding. The trans C≡N bond length in $(CN)_5Fe(NH_3)^{2-}$ appears to be the longest [1.168 (18) Å].[60] The average cis C≡N bond length is 1.142 (17) Å.[60] Unfortunately, the precision of these measurements is insufficient to be certain that the bond lengths are different. There is an internal consistency, however. The Fe–C(trans) bond length is shorter [1.89 (11) Å] than the Fe–C(cis) bond lengths [1.932 (8) and 1.945 (8) Å].[60] The difference between these bond lengths is $>3\sigma$. Ammonia is a weaker σ donor than imidazole (by $\sim^2/_5$).[37] The cyanide trans to ammonia can form a strong (short) σ bond (shorter than when trans to imidazole) and also receive more π^* electron density through back-bonding from Fe because NH_3 does not act as a π director. The C–N bond length becomes longer as the Fe–C bond length becomes shorter as expected.

An examination of the ligand bond lengths can also reveal evidence for π bonding in some cases. This is generally true, however, only for very small ligands such as CN^-, NO, and CO. Only when a very large amount of electron density is transferred to or from a larger ligand will significant bond length changes occur. Significant bond length changes have been reported for a coordinated flavin in a Ru^{2+} complex,[90] where extensive back-bonding is indicated.[91] If imidazole 1 of complex **3** donates a large amount of electron density to Fe, significant bond length changes should be observed. In particular, imidazole 1 should be different from imidazoles 2 and 3. This is not the case for most of the bond lengths. For each of the imidazoles the N_1–CH_3, C_4–C_5, N_3–C_4, and N_1–C_2 bond lengths are the same[92] within 2.7σ. Only two bond lengths are distinctly different from the corresponding bond lengths on the other imidazoles. The N_1–C_5 bond [N(11)–C(15)] of imidazole 3 is longer than the N_1–C_5 bonds of imidazoles 1 and 2. This longer bond may be associated with the out-of-plane methyl group on this $1\text{-}CH_3im$. The N_3–C_4–C_5 bond angle [N(10)–C(14)–C(15)] is also larger for imidazole 3, apparently as a result of the longer N_1–C_5 bond. The N_3–C_2 bond of imidazole 1 [N(6)–C(6) = 1.332 (3) Å] is 2.8σ longer than the next longest N_3–C_2 bond [imidazole 3, N(10)–C(16) = 1.318 (4) Å]. The length of this bond is even shorter for imidazole 2 [N(8)–C(10) = 1.305 (4) Å].

Imidazole 1 differs from imidazoles 2 and 3 for two bond angles. The N_1–C_2–N_3 angle of imidazole 1 [N(6)–C(6)–N(7)] is smaller than the corresponding angles of imidazoles 2 and 3. The C_5–N_1–C_2 angle of imidazole 1 [C(6)–N(7)–C(8)] is larger than the corresponding angles of imidazoles 2 and 3. This change of angles in imidazole 1 is just what is needed to accommodate the longer N_3–C_2 bond [N(6)–C(6)] and maintain a planar ring and aromaticity. Except for the N_3–C_4–C_5 angle, the ring bond angles of imidazoles 2 and 3 are also the same within experimental error.

The bond length and angle changes of imidazole 1 are consistent with π bonding from the imidazole to Fe. The N_3–C_2 bond is expected to be the most affected by π donation from the imidazole because it is the only bond that is affected by loss of electron density from both the π_1 and π_2 orbitals (see the MO diagrams of Figure 7).[24] Bond length changes of the imidazole are also possible from a σ induction toward the metal ion, but it is difficult to envision a mechanism that would localize this effect in one bond. This seems to be the first case where evidence for ligand-to-metal π bonding is observed from internal ligand bond length changes. It is important to note that crystals of **3** provide a unique opportunity to detect such small bond length changes because the same ligand also occurs in the structure in a non-π-bonding environment (imidazoles 2 and 3) for internal comparison. The crystal structures of several other $1\text{-}CH_3im$ complexes have been reported.[39b,67,93-99] The bond length data available for $1\text{-}CH_3im$ are collected in Table VII. Only two of the complexes for which data are available have a metal ion in an oxidation state that is

(90) Clarke, M. J.; Dowling, M. G.; Garafalo, A. R.; Brennan, T. F. *J. Am. Chem. Soc.* **1979**, *101*, 223–225.
(91) Benecky, M. J.; Dowling, M. G.; Clarke, M. J.; Spiro, T. G. *Inorg. Chem.* **1984**, *23*, 865–869.
(92) $\sigma = \sigma_{pool} = (\sigma_1^2 + \sigma_2^2)^{1/2}$. A bond length difference of 2.7 σ_{pool} (99% confidence level) or greater is considered significant. Glusker, J. P.; Trueblood, K. N. *Crystal Structure Analysis*, 2nd Ed.; Oxford University Press: New York, 1985; p 163.
(93) Scheidt, W. R.; Piciulo, P. R. *J. Am. Chem. Soc.* **1976**, *98*, 1913–1919.
(94) Jameson, G. B.; Rodley, G. A.; Robinson, W. T.; Gagne, R. R.; Reed, C. A.; Collman, J. P. *Inorg. Chem.* **1978**, *17*, 850–857.
(95) Jameson, G. B.; Molinaro, F. S.; Ibers, J. A.; Collman, J. P.; Brauman, J. I.; Rose, E.; Suslick, K. S. *J. Am. Chem. Soc.* **1980**, *102*, 3224–3237. See Table XII.
(96) Kirner, J. F.; Reed, C. A.; Scheidt, W. R. *J. Am. Chem. Soc.* **1977**, *99*, 2557–2563.
(97) Scheidt, W. R. *J. Am. Chem. Soc.* **1974**, *96*, 90–94.
(98) Momenteau, M.; Scheidt, W. R.; Eigenbrot, C. W.; Reed, C. A. *J. Am. Chem. Soc.* **1988**, *110*, 1207–1215.
(99) Little, R. G.; Ibers, J. A. *J. Am. Chem. Soc.* **1974**, *96*, 4452–4463.

favorable for imidazole π bonding: the Fe(III) centers of **3** and **4**. Both 1-methylimidazoles of **4** show the same bond lengths within experimental error[67] and are the same as for imidazole 1 of **3**. The second group of entries in the table are metal ions for which π bonding is not expected because of the low oxidation state—Mg(II), Mn(II), Fe(II), and Co(II). The N_3–C_2 bond lengths of **6** and **7** are shorter than the N_3–C_2 bond length of imidazole 1 of **3** by $>4.0\sigma$. The N_3–C_2 bond length of **6** is particularly short [1.295 (4) Å].[96] The Mn(II) of **6** is a high-spin d^5 ion. High-spin d^5 ions generally form ionic (noncovalent) bonds due, in part, to their zero crystal field stabilization energies.[100] The M–N(imidazole) bond length of **6** [2.192 (2) Å] is the longest of any first-row transition-metal–porphyrin–imidazole complex,[96] reflecting the large size of the high-spin d^5 Mn atom and the lack of covalency due to π bonding. This is consistent with the short N_3–C_2 bond of the coordinated 1-CH_3im in **6**. The Fe–N(1-CH_3im) bond of **7** is also long [2.180 (4) Å] even for an Fe(II)–N(imidazole) bond.[93,95] π bonding is expected for both of the low-spin Fe(III) cases [**3** (imidazole 1) and **4**], and the long N_3–C_2 bond is observed. No π bonding is expected for Mn(II), Mn(II), and low-spin Fe(II) [**3** (imidazoles 2 and 3), **6**, and **7**], and the short N_3–C_2 bond is observed. The length of the N_3–C_2 bond appears to be diagnostic of π bonding in ligated 1-CH_3im. The esd's of the other N_3–C_2 bond lengths in the second group of Table VII are too large to permit a definitive comparison, but all of the reported values are smaller than the values for the π-bonding group. The average N_3–C_2 bond lengths for the complexes capable of π bonding is 1.328 Å, while that of the complexes not expected to π bond with imidazole is 1.309 Å.

The data for complexes[101] **9**–**11** are included in the table even though the precision is very poor. These complexes [Fe(II) and Co(II)] are expected to have short N_3–C_2 bonds. The 1-CH_3im of **10** is highly disordered,[94] and the values for the bond lengths appear to be inaccurate. The N_1–CH_3 bond length of **11** disagrees with the other 11 values. The value of 1.41 (2) Å for the N_3–C_2 bond length of **11** is questionable. The bond length values of **6** and **10**–**12** are not included in the overall averages. We have tried to extend this correlation to other imidazoles; however, the precision of the bond length measurements of other low-spin Fe(III)–porphyrin–imH complexes is insufficient to draw conclusions.

Concluding Remarks

The evidence that 1-CH_3im is a π-donating ligand in **3** is summarized as follows. (1) The observation of a low-energy LMCT absorption indicates a small energy difference between the ligand π-donor and metal π-acceptor orbitals. (2) The observation of a large quadrupole splitting indicates a very nonspherical distribution of electron density consistent with the electron hole residing primarily in a single d orbital. (3) The Fe–N(imidazole) bond length is shortened by approximately twice the amount it would be, compared to a Fe–NH_3 bond length, if there were no π bonding. (4) The imidazole makes a ϕ angle of 34.5°, indicating an electronic effect due to π bonding. (5) The observation of a trans influence to shorten the C–N_{trans} cyanide bond length is consistent with the imidazole acting as a π director to align the electron hole in a single dπ orbital. (6) The lengthening of the N_3–C_2 bond is consistent with the removal of π-electron density from the imidazole.

Overall the π bonding is weak, however, on the basis of following. (1) The LMCT absorptions are weak, indicating poor orbital overlap. (2) Most of the stability of the Fe–N(imidazole) bond as measured by the association constant (K_f) comes from σ donation.[17] (3) The bond length changes of the coordinated imidazole are small.

Clearly, the electron-donating ability of imidazole (both σ and π) is important to the function of imidazole as a biological ligand. Imidazole can form strong bonds to a wide variety of metal ions for this reason. In cases where π bonding is involved, imidazole can exert an additional influence by strongly affecting the electron density distribution. The distribution can be modulated by changes in the M–imidazole bond length or orientation. Changes in the energy of the d_{xz} orbital will exert a variable trans influence and alter the oxidation–reduction potential and the preferred direction for electron transfer. In particular, raising the energy of d_{xz} puts more electron hole character into the ground state and alters numerous physicochemical properties. The structural analysis presented here cannot alone provide quantitative information about the nature of π bonding. Crystals of **3** are excellent candidates for studies by variable-temperature magnetic susceptibility, Mössbauer spectroscopy, polarized absorption spectroscopy, and ESR spectroscopy to determine the ground-state d-orbital wave functions and to develop a more detailed picture of imidazole π bonding.

Acknowledgment. We are grateful to Dr. Steve O'Donnell for assistance with the crystal structure determination and acknowledge support of this work from NIH Grant 1 R01 GM 30741-07. We also acknowledge support from Public Health Service Grant 1-S10-RR02381-01 for the Chemistry Department's X-ray diffraction laboratory. S.A.A. is an Established Investigator of the American Heart Association. This work was done during the tenure of an Established Investigatorship of the American Heart Association, Pennsylvania affiliate.

Supplementary Material Available: Tables S1–S4, listing hydrogen atom parameters, anisotropic thermal parameters, least-squares best planes, and dihedral angles, and Figures S1–S7, showing a stereoview of the molecular structure, four alternate perspective views of the structure, and a complete IR spectrum (13 pages); Table S5, listing observed and calculated structure factors (11 pages). Ordering information is given on any current masthead page.

(100) Lever, A. B. P. *Inorganic Electronic Spectroscopy*, 2nd ed.; Elsevier: New York, 1984; pp 448–451.

(101) Other 1-CH_3im structure determinations are cited in ref 98 [Zn(OEP)(1-CH_3im), Mn(TPP)(1-CH_3im)$_2^+$, and Fe(TPP)(1-CH_3im)$_2$], but the citations are to the abstract of a meeting and to a paper in press. These complexes are predicted to have N_3–C_2 bond lengths of ~1.309 Å on the basis of our work.